fgf8 mRNA decay establishes a gradient that couples axial elongation to patterning in the vertebrate embryo

Julien Dubrulle & Olivier Pourquié

Stowers Institute for Medical Research, 1000 East 50th Street, 64110 Kansas City, Missouri, USA

Formation and patterning of the vertebrate embryo occur in a head-to-tail sequence. This progressive mode of body formation from the posterior end of the embryo requires a strict temporal coordination of tissue differentiation—a process involving fibroblast growth factor (FGF) signalling. Here we show that transcription of *fgf8* messenger RNA is restricted to the growing posterior tip of the embryo. *fgf8* mRNA is progressively degraded in the newly formed tissues, resulting in the formation of an mRNA gradient in the posterior part of the embryo. This *fgf8* mRNA gradient is translated into a gradient of FGF8 protein, which correlates with graded phosphorylation of the kinase Akt, a downstream effector of FGF signalling. Such a mechanism provides an efficient means to monitor the timing of FGF signalling, coupling the differentiation of embryonic tissues to the posterior elongation of the embryo. In addition, this mechanism provides a novel model for morphogen gradient formation.

Posterior elongation of the vertebrate embryonic axis is driven initially by the blastopore closure or the regression of the node along the primitive streak and subsequently by the caudal movement of the tail bud. This particular developmental strategy gives rise to an apparent rostral-to-caudal wave of differentiation, whereby tissues located anteriorly are more advanced in their development than are tissues located posteriorly. This progression is well illustrated by the sequential production of somites from the paraxial mesoderm or by the rostro-caudal emigration wave of the neural crest from the neural tube.

Cells in the posterior-most tissues have been proposed to be maintained undifferentiated by a high level of FGF signalling and to activate their differentiation program only when they reach the appropriate threshold of FGF activity as they become located more distantly to the tail bud[1]. Much of this activity seems to be mediated by FGF8, which controls activation of the segmentation process in the presomitic mesoderm (PSM)[2,3] and onset of differentiation in the neural tube[4–6]. Because of the posterior elongation of the embryo, such a system implies a tight temporal control of FGF signalling in the newly formed posterior tissues. This requires that the highest activity of FGF signalling is constantly maintained in the newly produced cells of the posterior-most end of the embryo. In chick, *fgf8* transcripts show a graded distribution in the PSM and the adjacent neural tube, extending from the tail-bud area to the rostral third of the unsegmented region[3].

Graded distribution of FGF8 in the posterior embryo

Here, we first investigated whether the *fgf8* mRNA gradient can control the graded activation of the FGF pathway in the posterior embryo. *In situ* hybridization of mouse embryos with an *fgf8* probe indicated that, as in the chick embryo, *fgf8* is expressed in a graded fashion in the three germ layers (Fig. 1a–d, f–j). This suggests that the posterior *fgf8* mRNA gradient is a conserved feature among vertebrates. Examination of the cellular distribution of *fgf8* mRNA in the PSM gradient in chick and mouse embryos that had been stained for a short period of time clearly showed a salt-and-pepper expression pattern, indicating that the gradient is not smooth (Fig. 1e–j and Supplementary Fig. 1).

We used real-time polymerase chain reaction with reverse transcription (RT–PCR) to characterize further the shape of the *fgf8*

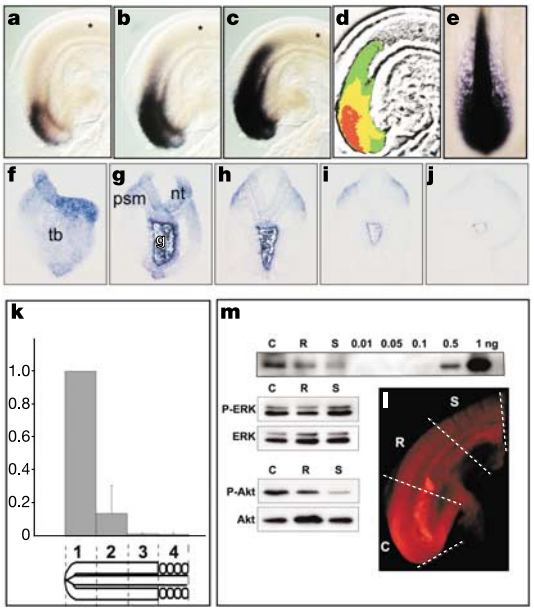

Figure 1 Characterization of the posterior gradient of *fgf8* mRNA and FGF8 protein. **a**–**c**, Tail region of the same E9.0 mouse embryo hybridized with an *fgf8* probe and photographed after increasing time in the staining reaction: 2 h (**a**), 4 h (**b**), 9 h (**c**). **d**, Overlay of the *fgf8* expression domains shown in **a**–**c**. **e**, Caudal region of a 2-day-old chick embryo hybridized with an *fgf8* probe after short development of the staining reaction to detect the salt-and-pepper expression pattern in the PSM. **f**–**j**, Progressively more anterior transverse cryosections of an E9.5 mouse embryo tail hybridized with an *fgf8* probe. **k**, Quantitative analysis of the amount of *fgf8* mRNA by real-time PCR in the four regions of the embryo indicated in the scheme below. **l**, Whole-mount immunohistochemistry on an E9.0 mouse tail probed with an antibody against FGF8. Hatched lines separate the three regions (C, R, S) of the posterior part of the embryo used for the biochemical analysis shown in **m**. **m**, Top, western blot of FGF8 in the regions indicated in **l**. The right part of the blot shows a concentration range (0.01–1 ng) of purified recombinant FGF8b. Bottom, phosphorylation state of ERK and Akt in the regions indicated in **l**. P-ERK and P-Akt denote the phosphorylated isoforms of the proteins. tb, tail bud; psm, presomitic mesoderm; nt, neural tube; g, hindgut. Asterisks in **a**–**c** indicate the last formed somite.

mRNA gradient in the mouse embryo. Four regions of equivalent size along the antero-posterior (AP) axis were delimited from the trunk of mouse embryos at embyonic day 9 (E9) to E10: three in the PSM, and one including the adjacent newly formed somites (Fig. 1k, bottom). The variation in the *fgf8* content of the four regions was then analysed by real-time RT–PCR and normalized to *Gapdh* (Fig. 1k, top). This analysis showed that the concentration of *fgf8* mRNA experiences a sharp drop-off in the rostral-PSM, indicating that the *fgf8* mRNA gradient in the caudal part of the embryo is not linear.

Depending on the rate of protein translation and on the stability and diffusion properties of the mature secreted protein, the final distribution of FGF8 protein need not necessarily be similar to that of its mRNA. To address this issue, we compared the distribution of *fgf8* mRNA and FGF8 protein in the mouse embryo. We first analysed the distribution of FGF8 protein along the AP axis of the murine embryo by immunohistochemical assessment of whole-mount embryos or parasagittal sections using a monoclonal antibody against the mouse FGF8 protein. This analysis showed that the protein is abundant in the tail bud and that its expression diminishes progressively caudo-rostrally in all three germ layers (Fig. 1l and data not shown).

Expression of FGF8 was assessed quantitatively by western blot analysis. Three regions of equivalent size along the AP axis were delimited from the trunk of E9–E10 mouse embryos (Fig. 1l): a region including the caudal half of the PSM (C), a region including the rostral half of the PSM (R), and a region including the adjacent newly formed somites (S). Protein extracts were prepared from pools of the three different regions described above and analysed. The FGF8 signal decreased in intensity in more rostral tissues (Fig. 1m).

We quantified the total amount of FGF8 protein in these three different regions of the embryo and found that the FGF8 concentration was of the order of 500 ng ml^{-1} (45 nM) in the caudal fragment. The FGF8 concentration progressively diminished rostrally to values in the somitic region that were between two- and fivefold lower than in the caudal-most region. These results indicate that the *fgf8* mRNA gradient is translated into a shallower protein gradient spanning a similar domain of the posterior mouse embryo. Given that the ED_{50} of FGF8b in a mitogenic assay linked to the number of cell divisions experienced by quiescent NR6R-3T3 cells is about 1–3 ng ml^{-1} and the dissociation constant (K_d) for the high-affinity FGF receptors is about 10^{-11} M, the observed concentrations in the caudal part of the embryo are within the physiological range and are consistent with a gradient of FGF8 activity in the PSM[7].

To examine this possibility, we monitored the phosphorylation state of extracellular-signal-regulated kinase (ERK) and Akt, two kinases involved in mediating the intracellular response downstream of FGF signalling through the Ras-dependent and phosphatidylinositol-3-OH kinase (PI(3)K)-dependent pathways, respectively[8]. No clear graded response of the phosphorylated isoforms of ERK was observed in mouse, consistent with immunocytochemical observations in the mouse primitive streak and PSM[9]. By contrast, the phosphorylated form of the Akt kinase clearly showed a graded profile with a strong signal in the unsegmented region, followed by a sharp decrease in the segmented region (Fig. 1m). These results are therefore consistent with the idea that the *fgf8* mRNA gradient is translated into a ligand gradient, which then controls a graded response along the AP axis in the caudal part of the embryo.

Gradient formation by *fgf8* mRNA decay

We examined how this gradient of mRNA is established and regulated during the course of axis elongation. The existence of a signal emitted by the tail end of the embryo that could activate *fgf8* transcription in a dose-dependent fashion would provide a plausible mechanism of linking axis regression and gradient formation. To test this hypothesis, we compared the expression of *fgf8* in explants of the posterior half of chick embryos with similar

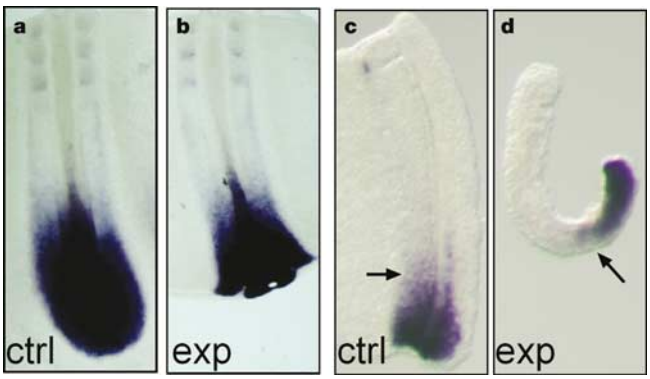

Figure 2 Expression of *fgf8* is not regulated by extrinsic signals. **a**, **b**, Posterior half explants of 17-somite stage chick embryos hybridized with an *fgf8* probe after a culture period of 210 min. **a**, Intact explant (ctrl); **b**, tail-bud ablation (exp). **c**, **d**, Intact left posterior half of a 2-day chick embryo (**c**) and contralateral isolated PSM (**d**), both cultured for 105 min and hybridized with an *fgf8* probe. Arrow, the rostral limit of *fgf8* expression in the PSM.

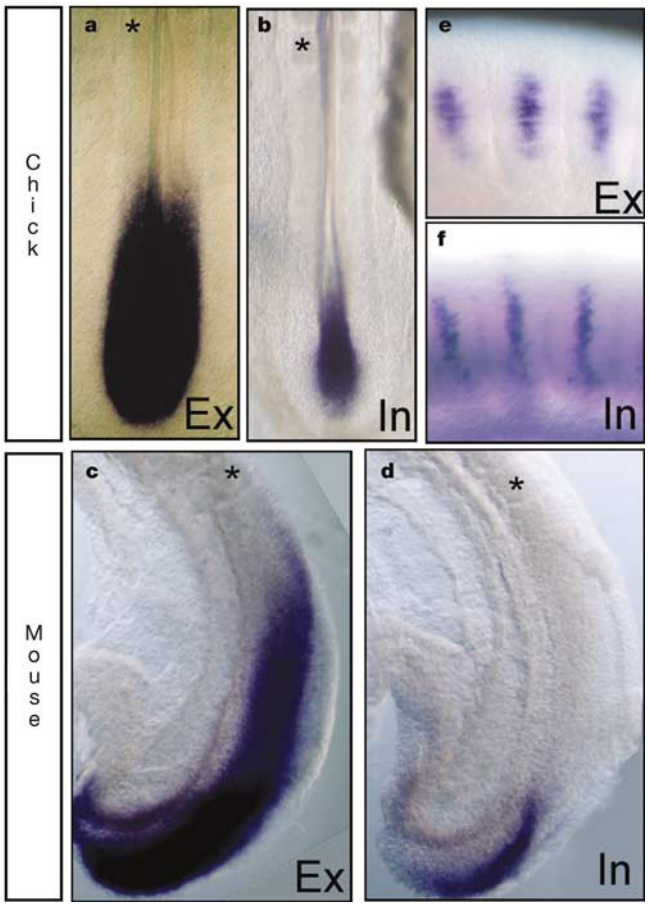

Figure 3 *fgf8* mRNA is only transcribed at the tail-bud level of mouse and chick embryos. Shown is a comparison of exonic (Ex) and intronic (In) *fgf8* expression in chick (**a**, **b**, **e**, **f**) and mouse (**c**, **d**) embryos. **a**, **b**, Embryonic tail region in 2-day-old chick embryos. **c**, **d**, Embryonic tail region in E9.5 mouse embryos. Asterisk, the last formed somite. **e**, **f**, Labelled myotomes from the trunk region in 3-day-old chick embryos.

explants in which the tail-bud region had been surgically removed (Fig. 2a, b). In the operated explants, the kinetics of the *fgf8* gradient regression was similar to that in the control explants, arguing against the requirement for a tail-bud-derived signal.

We further compared the regression of the *fgf8* mRNA gradient between explant cultures of isolated PSM dissected from one side of 2-day-old chick embryos with their intact contralateral half (Fig. 2c, d). After different culture periods, the intensity and rostral boundary of the *fgf8* expression domain were found to be similar between the dissected tissues and the intact embryonic halves, indicating that establishment of the gradient does not require signalling from the adjacent structures and is therefore an autonomous property of the caudal tissues.

An alternative mechanism based on progressive RNA decay could also account for the autonomous establishment of the caudal *fgf8* mRNA gradient. If *fgf8* mRNA transcription is restricted to the progenitor area in the tail bud and stops when cells become incorporated into the caudal-forming tissues derived from this area, then, taking into account the RNA degradation in these tissues, cells located more rostrally will contain less RNA than will cells that are located in the caudal part of the newly formed tissues (which have been more recently produced by the tail bud). To test this hypothesis, we monitored the production of *fgf8* nascent transcripts in chick and mouse embryos using riboprobes directed against intronic sequences of the *fgf8* gene (Fig. 3).

Whereas *fgf8* expression detected by the exonic probe was observed up to the rostral third of the unsegmented region in chicken embryos at the 20-somite stage (Fig. 3a), cells recognized by the intronic probe were strictly localized to the areas containing the paraxial mesoderm and neural tube progenitors of the tail bud (ref. 10 and Fig. 3b). A similar restriction of active *fgf8* transcription in the tail bud was observed in the mouse embryo (Fig. 3c, d). This difference in expression is not due to lower sensitivity of the intronic probe, because intronic expression was observed in virtually all known expression sites of exonic *fgf8*, such as the midbrain–hindbrain boundary, the myotome and the apical ectodermal ridge (AER) (Fig. 3f and data not shown). Nuclear expression of the intronic transcripts was particularly obvious in the chick myotome, where nuclei are aligned as a single stripe in the middle of the structure (compare Fig. 3f and e). These observations therefore suggest that the *fgf8* mRNA gradient seen in the caudal embryo does not result from active transcription but from the decay of mRNA transcribed at the level of the tail-bud progenitors.

To test this hypothesis further, we cultured the caudal portion of chick embryos at the 18–23-somite stage *in vitro* in medium containing the transcription inhibitor actinomycin D[11]. We then analysed the expression of mature *fgf8* transcripts by *in situ* hybridization after different times in culture. As a control, we monitored expression of the mature transcripts of *lunatic fringe* (*lfng*), a gene that has a rapid turnover of mRNA in the PSM under the same culture conditions[12]. Expression of *fgf8* transcripts in caudal tissues was still present and distributed in a graded fashion after incubation in actinomycin-D-containing medium for 3–5 h (Fig. 4a–c), whereas expression of *lfng* was totally abolished from embryos treated in the same conditions (Fig. 4d–f). Efficiency of the treatment was confirmed further by the absence of the *fgf8* expression that was initiated at the time of somite formation and later found in the posterior part of the somites in the treated embryos (Fig. 4a, arrow).

These results suggest that the *fgf8* transcripts detected in the caudal cells of the embryo did not derive from active transcription but instead were originally produced in the tail bud and inherited by their descendants in the PSM and the neural tube. The salt-and-pepper nature of *fgf8* mRNA within the gradient (Fig. 1e) is consistent with local cellular rearrangements that are known to occur in the posterior part of the embryo[13].

Discussion

Few cell divisions are observed in the PSM, suggesting that *fgf8* RNA decay along the AP axis is unlikely to result from massive clonal dilution[14]. Considering a constant rate of translation, therefore, the slope of the FGF8 protein gradient will be essentially controlled by the stability of the transcripts. Combined with the continuous production of committed cells caudally, these molecular mecha-

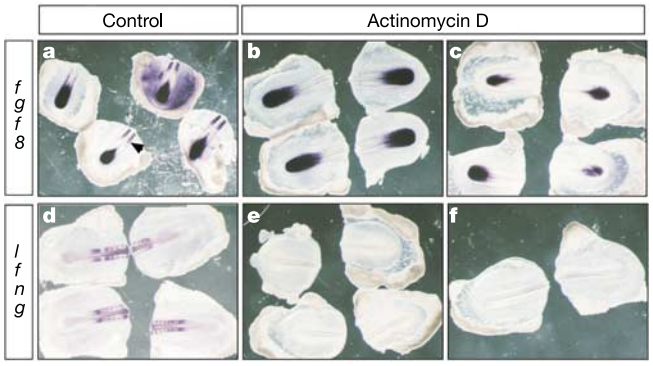

Figure 4 High stability of processed *fgf8* mRNAs. **a**–**f**, Posterior halves of chick embryos hybridized with exonic *fgf8* (**a**–**c**) or *lfng* (**d**–**f**) after *in vitro* culture in the absence (control) or presence of actinomycin D. **a**, **c**, **d**, **f**, After 5 h of culture; **b**, **e**, after 3 h of culture.

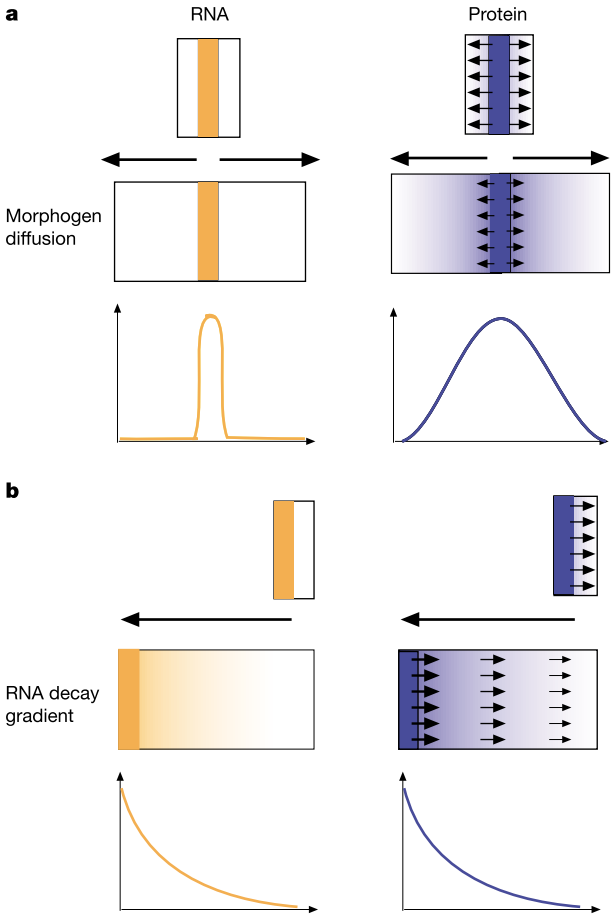

Figure 5 Two different mechanisms of establishing a protein gradient. **a**, Gradient formation by protein diffusion from a localized source. **b**, Gradient formation through polarized growth and mRNA decay.

nisms are indeed theoretically capable of generating a graded, dynamic distribution of a secreted molecule during elongation of the axis of the vertebrate embryo.

The establishment of gradients of secreted proteins during development have been studied mainly for morphogens such transforming growth factor-β or Wnt family members[15]. The formation of these gradients is described for systems undergoing even growth, and the gradients rely on the existence of a localized source producing the morphogen in the same place where the RNA transcription of the morphogen occurs (Fig. 5a).

The gradient is then established from the source across the developing field by specific diffusion properties of the protein or by active transport mechanism.

Our results provide evidence for a previously unrecognized mode of gradient formation in the embryo. In this model, the protein gradient is moulded onto the mRNA gradient, which is established owing to the peculiar polarized growth mode of the vertebrate axis (Fig. 5b). Such a patterning strategy of the embryonic axis might be used widely by other animals, such as invertebrates that show a sequential mode of development[16]. It might also be involved in the development of other embryonic structures arising by polarized growth, such as those derived from epithelial cords, as is seen in the development of many internal organs[17]. □

Methods

Plasmids and *in situ* hybridization

Whole-mount *in situ* hybridizations were done as described[18]. To generate intronic chick and mouse *fgf8* riboprobes, we first amplified the fourth intron of the *fgf8* gene by PCR on genomic DNA using the primers F (5′- GGAATTCATCTGCATGAACAAGAAGG-3′) and R (5′-GGAATTCACGCAGTCCTTGCCTTTGCCG-3′), and then cloned it into pGEMTeasy (Promega). The mouse fragment was further subcloned into pBluescript (Stratagene) after a *Pst*I–*Sac*I digestion to remove all flanking exonic sequences. The chick and mouse exonic *fgf8* and the *lfng* riboprobes have been described[12,19,20].

Real-time RT–PCR

Real-time RT–PCR analysis was done with the iCycler iQ detection system (Bio-Rad). In brief, E9.0 embryonic tails were cut in four equal parts (see Fig 1k), pooled in groups of two, and subjected to total RNA extraction by the RNeasy minikit (Qiagen). Each RNA sample was divided into two and subjected to RT–PCR for *fgf8* and *Gadph* within the same run using Quantitect SYBR Green buffer (Qiagen). We used the following primers: for *fgf8*, F (5′-CAGCTCTACAGCCGCACCAGC-3′) and R (5′-TGCTCTTGGCAATTAGC TCC-3′); for *Gadph*, F (5′-AACGACCCCTTCATTGAC-3′) and R (5′-TCCACGACATAC TCAGCAC-3′).

Before real-time RT–PCR, the quality and purity of amplified fragments, as well as protocol optimization, were checked after traditional RT–PCR by agarose gel electrophoresis. Results are presented as the fold expression of *fgf8* relative to the caudal-most part of the tail, which was calculated using $2^{-\mathrm{dd}Ct}$, where $\mathrm{d}C_t = fgf8\ C_t - Gadph\ C_t$ and $\mathrm{dd}C_t = \mathrm{d}C_t$ of the caudal part $-\mathrm{d}C_t$ of a given region[21]. The C_t value is the calculated threshold cycle number at which the fluorescent signal is significantly above the background. The graph in Fig. 1k plots the mean ± s.d. of the fold expression of each of the four regions from a total of six embryos.

FGF8 protein detection

Immunohistochemistry was done by standard procedures using a monoclonal antibody against FGF8b (R&D Systems), a biotinylated antibody against mouse IgG1 (Southern Biotech) and Cy3-conjugated streptavidin (Sigma).

Western blot analysis was done by standard procedures. The caudal region of mouse embryos at the 20–30-somite stage was divided into three equal parts (see Fig. 1l) corresponding to the caudal half, the rostral half of the unsegmented region and a region including the last formed somites. We lysed samples in RIPA buffer containing 1 mM NaF, 1 mM Na_3VO_4, 1 mM sodium pyrophosphate and Complete proteases inhibitor cocktail (Roche). Proteins were extracted from pools of the different regions and separated by SDS–PAGE on 12% acrylamide gels. The concentration of FGF8 in tissue was evaluated by comparing signal intensity in the embryo samples (normalized to β-actin) to known dilutions of recombinant mouse FGF8b (R&D Systems).

The FGF8 signal intensity was quantified either from the autoradiogram after detection by electrochemiluminescence (Amersham) using Image software (NIH) and normalization to the expression of β-actin (A-2066, Sigma) ($n = 8$), or by western blotting using Alexa-coupled secondary antibodies and a Li-cor scanning system ($n = 3$). Both methods gave similar estimations. Antibodies against ERK (9101), phosphorylated ERK (9102), Akt (9272) and phosphorylated Akt (9271) were from Cell Signalling Technology, and western blots were done in accordance with the manufacturer's instructions. Western blots were reproduced at least three times for each antibody.

In vitro chick embryo culture and actinomycin D treatment

Chick embryo explants at the 18–23-somite stage were cultured *in vitro* as described[3]. In a first series of experiments, intact posterior half explants and posterior half explants where the tail-bud region was surgically removed were cultured in parallel for up to 230 min. In a second series, isolated PSM and contralateral intact half embryos were cocultured for 60–270 min. In a third series, intact posterior half embryos were cultured in the presence or absence of 5 or 10 $\mu g\,ml^{-1}$ actinomycin D (Sigma) for up to 5 h. We then fixed the explants for *in situ* hybridization.

Received 7 July; accepted 5 November 2003; doi:10.1038/nature02216.

1. Vasiliauskas, D. & Stern, C. D. Patterning the embryonic axis: FGF signaling and how vertebrate embryos measure time. *Cell* **106,** 133–136 (2001).
2. Sawada, A. *et al.* Fgf/MAPK signalling is a crucial positional cue in somite boundary formation. *Development* **128,** 4873–4880 (2001).
3. Dubrulle, J., McGrew, M. J. & Pourquié, O. FGF signaling controls somite boundary position and regulates segmentation clock control of spatiotemporal Hox gene activation. *Cell* **106,** 219–232 (2001).
4. Mathis, L., Kulesa, P. M. & Fraser, S. E. FGF receptor signalling is required to maintain neural progenitors during Hensen's node progression. *Nature Cell Biol.* **3,** 559–566 (2001).
5. Diez del Corral, R., Breitkreuz, D. N. & Storey, K. G. Onset of neuronal differentiation is regulated by paraxial mesoderm and requires attenuation of FGF signalling. *Development* **129,** 1681–1691 (2002).
6. Bertrand, N., Medevielle, F. & Pituello, F. FGF signalling controls the timing of Pax6 activation in the neural tube. *Development* **127,** 4837–4843 (2000).
7. Chellaiah, A., Yuan, W., Chellaiah, M. & Ornitz, D. M. Mapping ligand binding domains in chimeric fibroblast growth factor receptor molecules. Multiple regions determine ligand binding specificity. *J. Biol. Chem.* **274,** 34785–34794 (1999).
8. Schlessinger, J. Cell signaling by receptor tyrosine kinases. *Cell* **103,** 211–225 (2000).
9. Corson, L. B., Yamanaka, Y., Lai, K. M. & Rossant, J. Spatial and temporal patterns of ERK signaling during mouse embryogenesis. *Development* **130,** 4527–4537 (2003).
10. Catala, M., Teillet, M. A. & Le Douarin, N. M. Organization and development of the tail bud analyzed with the quail–chick chimaera system. *Mech. Dev.* **51,** 51–65 (1995).
11. Hyman, R. W. & Davidson, N. Kinetics of the *in vitro* inhibition of transcription by actinomycin. *J. Mol. Biol.* **50,** 421–438 (1970).
12. McGrew, M. J., Dale, J. K., Fraboulet, S. & Pourquié, O. The *lunatic fringe* gene is a target of the molecular clock linked to somite segmentation in avian embryos. *Curr. Biol.* **8,** 979–982 (1998).
13. Kulesa, P. M. & Fraser, S. E. Cell dynamics during somite boundary formation revealed by time-lapse analysis. *Science* **298,** 991–995 (2002).
14. Stern, C. D., Fraser, S. E., Keynes, R. J. & Primmett, D. R. A cell lineage analysis of segmentation in the chick embryo. *Development* **104,** 231–244 (1988).
15. Gurdon, J. B. & Bourillot, P. Y. Morphogen gradient interpretation. *Nature* **413,** 797–803 (2001).
16. Davis, G. K. & Patel, N. H. The origin and evolution of segmentation. *Trends Cell Biol.* **9,** M68–M72 (1999).
17. Hogan, B. L. & Kolodziej, P. A. Organogenesis: molecular mechanisms of tubulogenesis. *Nature Rev. Genet.* **3,** 513–523 (2002).
18. Henrique, D. *et al.* Expression of a Delta homologue in prospective neurons in the chick. *Nature* **375,** 787–790 (1995).
19. Crossley, P. H. & Martin, G. R. The mouse Fgf8 gene encodes a family of polypeptides and is expressed in regions that direct outgrowth and patterning in the developing embryo. *Development* **121,** 439–451 (1995).
20. Crossley, P. H., Minowada, G., MacArthur, C. A. & Martin, G. R. Roles for FGF8 in the induction, initiation, and maintenance of chick limb development. *Cell* **84,** 127–136 (1996).
21. Bottone, F. G. Jr, Martinez, J. M., Collins, J. B., Afshari, C. A. & Eling, T. E. Gene modulation by the cyclooxygenase inhibitor, sulindac sulfide, in human colorectal carcinoma cells: possible link to apoptosis. *J. Biol. Chem.* **278,** 25790–25801 (2003).

Supplementary Information accompanies the paper on **www.nature.com/nature**.

Acknowledgements We thank D. Duboule for discussions; G. Martin for reagents; B. Brede for help with real-time PCR; S. Fraser , D. Ish-Horowicz, P Kulesa, T. Lecuit and members of the Pourquié laboratory for comments on the manuscript. J.D. was a recipient of a fellowship from the Fondation pour la Recherche Medicale (FRM). This work was initiated in the Laboratoire de Genetique et Physiologie du Developpement in Marseille, supported by funding from the Centre National de le Recherche Scientifique (CNRS), Human Frontier Science Program Organization (HFSPO), Association Francaise contre les Myopathies and the Université de la Méditerranée-AP de Marseille. Current work is supported by the Stowers Institute and a grant from the NIH.

Competing interests statement The authors declare that they have no competing financial interests.

Correspondence and requests for materials should be addressed to O.P. (olp@stowers-institute.org).